HIGH TECHNOLOGY LETTERS | Vol. 27 No. 4 | Dec. 2021 | pp. 337-346

doi:10.3772/j.issn.1006-6748.2021.04.001

On the performance of full-duplex non-orthonogal multiple access with energy harvesting over Nakagami-m fading channels[①]

Guo Weidong (郭卫栋)[②*,**], Zheng Dong[*]

([*] School of Information Science and Engineering, Shandong University, Qingdao 266237, P. R. China)

([**] School of Cyber Science and Engineering, Qufu Normal University, Qufu 273165, P. R. China)

Abstract

A cooperative full-duplex (FD) non-orthogonal multiple access (NOMA) network is considered, in which a source communicate with multiple users via multiple energy harvesting (EH) FD relays. Based on this structure, a novel relay selection scheme is proposed over Nakagami-m fading channels by considering both the channel state information (CSI) and the energy statuses of relays. A finite Markov chain is adopted to capture the evolution of relay batteries and simplify the performance analysis by making some reasonable assumptions. General closed-form expressions of the outage probability and the ergodic sum-rate are derived. All the theoretical results are validated by Monte-Carlo simulations. The impacts of various system parameters, such as the number of relays, the self-interference (SI) at the involved relay and battery size, on the performance are extensively investigated. It is shown that the usage of NOMA with FD relaying outperforms the half-duplex (HD)-NOMA and conventional orthogonal multiple access (OMA) network when the self-interference is not too large.

Key words: non-orthogonal multiple access (NOMA), full-duplex (FD), energy harvesting (EH), Markov chain

0 Introduction

As one of the promising key techniques of the fifth generation (5G) wireless networks, non-orthogonal multiple access (NOMA) has been applied in various areas[1-2]. NOMA utilizes the power domain to achieve multiple-access strategies, which is unlike the conventional orthogonal multiple access (OMA) structures. Since the NOMA technique exploits the new dimension of the power domain, it has the potential to be integrated with existing MA paradigms. On the other hand, the technique of cooperative transmission can form a virtual multiple-input multiple-output (MIMO) scheme to process data cooperatively, which can enhance the communication reliability for the users who are in poor channel conditions. It is reasonable to integrate NOMA into relaying networks. Ref. [3] proposed a new cooperative NOMA scheme and analyzed the outage probability and diversity gain of the system. In Ref. [4], it is revealed that cooperative NOMA achieves the same diversity order and the superior coding gain compared to cooperative OMA.

To avoid additional bandwidth cost for cooperative NOMA system, full-duplex (FD) has attracted considerable attention, because transmission and reception are performed simultaneously on the same carrier frequency in FD operation[5]. Two main types of FD relay techniques, namely FD amplify-and-forward (AF) relaying and FD decode-and-forward (DF) relaying, had been discussed in Refs [6-8]. The outage probability of FD-AF relaying with a non-negligible direct link was analyzed in Ref. [6], which considers the processing delay of relaying in practical scenarios. Ref. [7] analyzed the outage probability of a basic three-node FD-AF relaying system. Ref. [8] characterized the outage performance of FD-DF relaying and demonstrated that it is possible to determine which duplex mode is superior under the target outage probability.

Another goal of 5G networks is to maximize the energy efficiency. Therefore, energy harvesting (EH), a technique to harvest energy from radio frequency signals, has received considerable attention as a solution to overcome the bottleneck of energy constrained system[9]. Recently, relays with EH capabilities have attracted lots of research interests, where the relay can

① Supported by the National Natural Science Foundation of China (No. 61901245).

② To whom correspondence should be addressed. E-mail: gud2001@qfnu.edu.cn

Received on Feb. 2, 2021

use the energy harvested from the other nodes to perform the data forwarding[10]. This can solve the problem of the energy supply of relays and expand the application of EH-based wireless communications. Ref. [11] investigated a dual-hop cooperative communication system, where source node communicates with destination node through direct and EH relaying paths. Ref. [12] addressed energy efficiency-spectrum efficiency trade-off in an EH cooperative cognitive radio network operated in a frame structure comprising of spectrum sensing and cooperation-transmission mode. Nevertheless, the amount of energy harvested from RF radiation is often restricted and it is desirable for relays to accumulate the harvested energy in the energy storage such as super-capacitors or rechargeable batteries[13]. In Ref. [14], different from the conventional battery-free EH relaying strategy, harvested energy is prioritized to power information relaying while the remainder is accumulated and stored for future usage with the help of a battery in the proposed strategy, which supports an efficient utilization of harvested energy.

In order to improve the spectral efficiency and energy efficiency, the FD-NOMA relaying for the downlink transmission over Nakagami-*m* fading channels is considered and a comprehensive performance analysis is provided. The analysis of this paper provides more general results, as the Nakagami-*m* fading can incorporate the most commonly used Rayleigh fading and Rice fading as special cases, which can be obtained by adjusting the fading parameter. The main contributions of this paper are summarized as follows.

(1) This paper studies a NOMA-based downlink FD-AF relaying network over Nakagami-*m* fading channels. The relays have no other energy supplies, but they are equipped with chargeable battery and can harvest and store the wireless energy broadcasted by the source. Based on this structure, a new relay selection scheme is proposed considering both the channel state information (CSI) and the battery statuses of relays.

(2) This model combines NOMA, cooperative communication, FD and EH together reasonably and can improve spectral efficiency and energy efficiency simultaneously.

(3) The amount of energy stored in the battery of each relay is modeled as finite states and a finite Markov chain is used to model the variation of energy at each relay. Both the transition probability and the steady-state probability are derived for the next performance analysis.

(4) The asymptotic expressions of outage probability and the ergodic sum-rate for both near and far users are derived. Finally, simulation results are presented to validate the theoretical analysis and verify the superiority of FD-NOMA relaying over the traditional HD-NOMA relaying and OMA relaying.

This paper is different from the recent work[15]. The main differences between them are summarized as follows.

(1) The models of two papers are quite different. In Ref. [15], the model is very simple. The source has no direct link with users. The channels are assumed to follow Rayleigh fading and relays operate in half-duplex mode. In this paper, the source has direct link with users and the channels are assumed to follow Nakagami-*m* fading which is more accorded with actual communication scenarios. In addition, relays in this paper operate in full-duplex mode which improves the spectral efficiency.

(2) In Ref. [15], the source transmits information to all users simultaneously using NOMA scheme. While in this paper, 2-user NOMA is used. In general, 2-user NOMA is a typical scenario, where two of all users are selected to perform NOMA. The decoding complexity and delay at the receivers are lower and shorter compared with all-user NOMA.

(3) In Ref. [15], only outage probability is analyzed, while in this paper, both outage probability and ergodic sum-rate are analyzed.

The rest of this paper is organized as follows. System model is introduced in Section 1. The relay selection scheme is illustrated in Section 2. The closed-form expressions of outage probability and ergodic sum-rate are derived in Section 3. Numerical and simulations results are presented in Section 4 and conclusions are drawn in Section 5.

1 System model

As shown in Fig. 1, in the proposed system, a source S intends to communicate to a number of potential users $D_j (j = 1, 2, \cdots, N)$ over channels with flat fading. Multiple potential FD relays $R_i (i = 1, 2, \cdots, M)$ are willing to amplify and forward the signal from S to the users. It is assumed that there exist direct links between S and users. S and D_j are configured with one antenna and operate in HD mode, while relays are equipped with one transmit antenna and one receive antenna that enables an FD operation. The channel between any transmitter and any receiver is assumed to follow Nakagami-*m* fading. The channels pertaining to the direct link, first hop and second hop undergo independent identically (i. i. d.) fading and the channel coefficients are denoted by h_{SD_j}, h_{SR_i} and $h_{R_iD_j}$ with parameters m_0, m_1 and m_2, respectively. The channel power gains $G_{SD_j} = |h_{SD_j}|^2$, $G_{SR_i} = |h_{SR_i}|^2$ and $G_{R_iD_j} = |h_{R_iD_j}|^2$ thus follow the Gamma distribution, with mean Φ_{SD}, Φ_{SR} and Φ_{RD}, respectively.

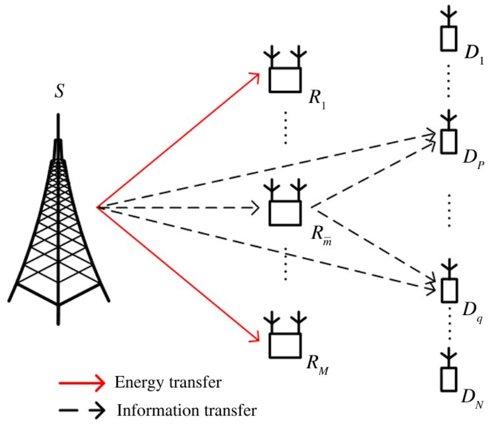

Fig. 1 A reference model for multi-relay cooperative FD-NOMA network

In a general case, due to the imperfect isolation or cancellation process, FD operation may suffer from residual self-interference (SI). In order to simplify the analysis, it is assumed that each relay with spatially separated transmit and receive antennas is fixed, and the interference channel is non-fading, where the instantaneous interference-to-noise ratio (INR) equals the corresponding average INR. As shown later in the simulations, this assumption does not degrade the accuracy of our analysis. Without loss of generality, the users' channel gains are assumed to be ordered as $\hat{G}_{SD_1} \leqslant \hat{G}_{SD_2} \leqslant \cdots \leqslant \hat{G}_{SD_N}$ ($\hat{G}_{SD_j}$ is the sorted random variable of G_{SD_j}). In what follows, it is focused on the analysis of the group users consisting of D_p and D_q ($\hat{G}_{SD_p} < \hat{G}_{SD_q}$). It is also assumed that the additive white Gaussian noise (AWGN) of all links has a zero mean and equal variance σ^2.

AF-NOMA protocol is used for downlink transmission and a normalized unit block time (i.e., $T = 1$) is considered. Before the transmission, each relay judges if it has enough energy to forward the information. If the relay does not have enough energy, it performs EH in this time block and stores the harvested energy into its battery. The amount of energy harvested from the source can be expressed as

$$\omega_{R_i} = \eta P_S G_{SR_i} T \tag{1}$$

where, P_S is the source power, η is the energy harvesting efficiency at each relay.

For those relays with sufficient energy, they report their CSI to S for the relay selection decision. Letting ω_i denote the amount of energy in the battery of relay R_i, relays with enough energy are defined as the eligible set

$$\xi = \{R_i \mid \omega_i > VC,\ i = 1,2,\cdots,M\} \tag{2}$$

where, C is the energy harvesting threshold to activate the EH circuit, V is a positive integer. If the selected relay for forwarding data is assumed to have the same transmitting power as S, V must satisfy

$$(V-1)C < P_S T < VC \tag{3}$$

Among this set of relays, $R_{\bar{m}}$ is selected, which can be expressed as

$$\bar{m} = \arg\max_{i:R_i \in \xi} \{G_{SR_i}\} \tag{4}$$

In Eq. (4), the relay with the best channel power gain of the first hop in ξ is selected for forwarding the information, all other relays perform EH in this block time. It is assumed that the transmitting power of the selected relay ($P_{R_{\bar{m}}}$) is the same as S, which means $P_S = P_{R_{\bar{m}}} = P$. Although the energy consumed of $R_{\bar{m}}$ for sending data in one block time is PT, which can be seen from Eq. (3), it is still considerd that the energy consumption for transmission as VC, because C is the basic unit of the relay battery. The difference between PT and VC does not severely degrade the accuracy of the performance analysis.

After selection, S broadcasts the signal $x_S[k] = \sqrt{a_p}x_p[k] + \sqrt{a_q}x_q[k]$ (a_p and a_q are the power allocation factors and satisfy $a_p + a_q = 1$, $a_p > a_p$). While the selected relay $R_{\bar{m}}$ simultaneously receives $x_s[k]$ and forwards the signal generated by co-channel transmission to D_p and D_q in FD mode, and the corresponding D_p and D_q simultaneously receive signals forwarded by the relay $R_{\bar{m}}$ and transmitted from S. In the kth time slot ($k = 1, 2, 3, \cdots$), the signals received at $R_{\bar{m}}$, D_p and D_q can be written by

$$\begin{aligned} y_{R_{\bar{m}}}[k] &= h_{SR_{\bar{m}}}\sqrt{P}x_S[k] + h_{RR_{\bar{m}}}\sqrt{P}Ay_{R_{\bar{m}}}[k - T_d] \\ &\quad + n_{R_{\bar{m}}}[k] \end{aligned} \tag{5}$$

$$\begin{aligned} y_{D_p}[k] &= h_{SD_p}\sqrt{P}x_S[k] + h_{R_{\bar{m}}D_p}\sqrt{P}Ay_{R_{\bar{m}}}[k - T_d] \\ &\quad + n_{D_p}[k] \end{aligned} \tag{6}$$

$$\begin{aligned} y_{D_q}[k] &= h_{SD_q}\sqrt{P}x_S[k] + h_{R_{\bar{m}}D_q}\sqrt{P}Ay_{R_{\bar{m}}}[k - T_d] \\ &\quad + n_{D_q}[k] \end{aligned} \tag{7}$$

where, A is the amplification coefficient, $h_{RR_{\bar{m}}}$ is residual SI between transmit antenna and receive antenna of relay, and T_d is the processing delay. $n_{R_{\bar{m}}}[k]$, $n_{D_p}[k]$ and $n_{D_q}[k]$ are AWGNs. Without loss of generality and for overall simplicity, it is assumed that $\gamma = P/\sigma^2$ is the average signal to noise ratio (SNR). $\gamma_{\bar{m}} = \gamma|h_{RR_m}|^2$ is set as an actual measured value, which averages out the fading effect. With unity energy transmit signals and after some simple substitutions, A can be expressed as[16]

$$A = (G_{SR_{\bar{m}}} P + | h_{RR_{\bar{m}}} |^2 P + \sigma^2)^{-\frac{1}{2}} \quad (8)$$

In this study, it is supposed that the two signals from S and $R_{\bar{m}}$ are resolvable absolutely (herein the relaying link corresponding to direct link has small time delay for any transmitted signals, the same as in Ref. [17]). After some simplification, the instantaneous signal-to-interference- plus-noise-ratios (SINRs) at D_p from S and $R_{\bar{m}}$ are expressed by

$$\gamma_{SD_p} = \frac{a_p \hat{G}_{SD_p} \gamma}{a_q \hat{G}_{SD_p} \gamma + 1} \quad (9)$$

$$\gamma_{R_{\bar{m}}D_p} = \frac{a_p \gamma^2 G_{SR_{\bar{m}}} G_{R_{\bar{m}}D_p}}{\gamma(G_{SR_{\bar{m}}} + G_{R_{\bar{m}}D_p}) + \gamma G_{R_{\bar{m}}D_p}(a_q \gamma G_{SR_{\bar{m}}} + \gamma_{\bar{m}}) + \gamma_{\bar{m}} + 1} \quad (10)$$

Using selection combining (SC), the instantaneous SINR of D_p can be obtained as

$$\gamma_{D_p} = \max(\gamma_{SD_p}, \gamma_{R_{\bar{m}}D_p}) \quad (11)$$

As for D_q, the successive interference cancellation (SIC) is applied to decode information of D_p. Particularly, D_q first decodes the message of D_p, then subtracts this component from the received signal to detect its own information. Therefore, the received SINRs at D_q for the decoding of the information of D_p are given by

$$\gamma_{SD_{q\to p}} = \frac{a_p \hat{G}_{SD_q} \gamma}{a_q \hat{G}_{SD_q} \gamma + 1} \quad (12)$$

$$\gamma_{R_{\bar{m}}D_{q\to p}} = \frac{a_p \gamma^2 G_{SR_{\bar{m}}} G_{R_{\bar{m}}D_q}}{\gamma(G_{SR_{\bar{m}}} + G_{R_{\bar{m}}D_q}) + \gamma G_{R_{\bar{m}}D_q}(a_q \gamma G_{SR_{\bar{m}}} + \gamma_{\bar{m}}) + \gamma_{\bar{m}} + 1} \quad (13)$$

After SIC operation, the instantaneous SINRs at D_q for the decoding of its own information are expressed by

$$\gamma_{SD_q} = a_q \hat{G}_{SD_q} \gamma \quad (14)$$

$$\gamma_{R_{\bar{m}}D_q} = \frac{a_q \gamma^2 G_{SR_{\bar{m}}} G_{R_{\bar{m}}D_q}}{\gamma(G_{SR_{\bar{m}}} + G_{R_{\bar{m}}D_q}) + \gamma G_{R_{\bar{m}}D_q} \gamma_{\bar{m}} + \gamma_{\bar{m}} + 1} \quad (15)$$

Similar to Eq. (11), according to the SC, the instantaneous SINR of D_q can be expressed as

$$\gamma_{D_q} = \max(\gamma_{SD_q}, \gamma_{R_{\bar{m}}D_q}) \quad (16)$$

2 Relay selection rule

At the beginning of a transmission block, each relay checks its battery and judges whether it has enough energy to forward the information. For those relays with sufficient energy, they report their CSI to S for making the relay selection decision. All other relays apart from $R_{\bar{m}}$ perform EH in this block time. If no relay has enough energy, all relays perform EH in this block time. It is assumed that each relay accumulates the harvested energy using a finite energy storage with the size BC ($B = 1, 2, 3, \cdots$). The relay can harvest uC amount of energy in one block and u is given by

$$uC \leqslant \omega_{R_i} < (u + 1)C \quad u = (1, 2, 3, \cdots) \quad (17)$$

This assumption is closer to the practical scenario, and the evolution of the battery status of each relay can be modeled as a finite-state Markov chain. Using the transition probability matrix of this chain, the steady state probability vector which can be used for analyzing the performance can be got.

The above analysis is computationally intense when M is large. To facilitate the computation, an approximated approach based on two simplified assumptions is proposed. Firstly, the relay energy amount at the selection epoch is denoted as a random variable Z. To ease the computation, Z is approximated as a uniform random variable over $[0, BC]$. This approximation is inspired by considering the amount of harvested energy in a transmission block follows the geometric distribution with parameter 1/2[18]. The effectiveness of the assumption will be discussed in the simulation part. Secondly, it is easy to find that each relay may be either short of enough energy to participate in relay selection or otherwise, so the evolution of relay energy amount is captured by using two states, either active or inactive. With this two-state Markov chain, a relay is in s_0 if the relay lacks sufficient energy to transmit, or in s_1 when the relay has enough energy for transmission. Next, how to obtain the transition probability matrix of this two-state Markov chain will be discussed.

The transition from s_0 to s_0 happens when a relay has no enough energy to transmit (i. e., $Z < VC$) in the current block and the accumulated energy after harvesting remains below VC. The corresponding transition probability is given by

$$\begin{aligned} p_{0,0} &= \Pr(Z + \omega_{R_i} < VC \mid 0 \leqslant Z < VC) \\ &= \Pr(\hat{Z} + \omega_{R_i} < VC) \end{aligned} \quad (18)$$

where, $\hat{Z}$ is a truncated random variable defined as

$$\hat{Z} = \begin{cases} Z & Z < VC \\ 0 & Z \geqslant VC \end{cases} \quad (19)$$

Since Z is approximated as uniformly distributed, the probability density function (PDF) of $\hat{Z}$ can be obtained as

$$f_{\hat{Z}}(z) = \frac{1}{BC} u(VC - z) + \left(1 - \frac{V}{B}\right) \delta(z - VC) \quad (20)$$

where, $u(\cdot)$ and $\delta(\cdot)$ denote the unit step function and the Dirac delta function, respectively. Considering the channels obey Nakagami-m distribution, a general random variable G_{SR_i}, is subjected to a Gamma distribution, the corresponding PDF is

$$f_{G_{SR_i}}(x) = \left(\frac{m_1}{\Phi_{SR}}\right)^{m_1} \frac{x^{m_1-1}}{\Gamma(m_1)} \exp\left(-\frac{m_1 x}{\Phi_{SR}}\right) \quad (21)$$

where $\Gamma(\cdot)$ is Gamma function[19]. The corresponding cumulative distribution function (CDF) is expressed by

$$F_{G_{SR_i}}(x) = 1 - \exp\left(-\frac{m_1 x}{\Phi_{SR}}\right) \sum_{n=0}^{m_1-1} \frac{(m_1 x/\Phi_{SR})^n}{n!} \quad (22)$$

If m_1 takes positive integer value, then with the help of Ref. [19], Eq. (18) can be solved as

$$p_{0,0} = \int_0^{VC} \Pr\left(G_{SR_i} < \frac{VC - z}{\eta VC}\right) f_{\hat{Z}}(z)\,\mathrm{d}z = 1 - \frac{1}{BC} \sum_{n=0}^{m_i-1} \left(\frac{1}{m_1/\overline{\omega}_{R_i}} - \exp\left(-\frac{m_1 VC}{\overline{\omega}_{R_i}}\right) \sum_{k=0}^{n} \frac{n!(VC)^k}{k!(m_1/\overline{\omega}_{R_i})^{1-k}}\right) \quad (23)$$

where $\overline{\omega}_{R_i} = E(\omega_{R_i}) = VC\eta\Phi_{SR}$.

The transition from s_0 to s_1 happens when the relay enters the EH mode in the current bock and the accumulated energy exceeds VC. Hence,

$$p_{0,1} = \Pr(Z + \omega_{R_i} \geqslant VC \mid 0 \leqslant Z < VC) = \Pr(\hat{Z} + \omega_{R_i} \geqslant VC) \quad (24)$$

Similar to the derivation of Eq. (22), Eq. (25) can be obtained.

$$p_{0,1} = \frac{1}{BC} \sum_{n=0}^{m_1-1} \left(\frac{1}{m_1/\overline{\omega}_{R_i}} - \exp\left(-\frac{m_1 VC}{\overline{\omega}_{R_i}}\right) \sum_{k=0}^{n} \frac{n!(VC)^k}{k!(m_1/\overline{\omega}_{R_i})^{1-k}}\right) \quad (25)$$

The transition from s_1 to s_0 happens when the relay with enough energy is selected as the best relay for transmitting and its remaining energy is not enough for another transmitting. Hence, the transition probability is given by

$$p_{1,0} = \Pr(Z - VC < VC \mid VC \leqslant Z \leqslant BC) \Pr(R_{\bar{m}} = R_i) = \Pr(\tilde{Z} < 2VC) \Pr(R_{\bar{m}} = R_i) \quad (26)$$

where, $\tilde{Z}$ is a truncated random variable defined as

$$\tilde{Z} = \begin{cases} Z & VC \leqslant Z \leqslant BC \\ 0 & Z < VC \end{cases} \quad (27)$$

Since Z is uniformly distributed, the PDF of $\tilde{Z}$ can be obtained as

$$f_{\tilde{Z}}(z) = \frac{1}{BC}(u(z - BC) - u(z - VC)) + \frac{W}{B}\delta(z - VC) \quad (28)$$

Using this PDF, the first term in the right of Eq. (26) can be obtained as

$$\Pr(\tilde{Z} < 2VC) = \begin{cases} 2V/B & 2VC < BC \\ 1 & 2VC \geqslant BC \end{cases} \quad (29)$$

As to the second term, it is noted that the i. i. d. fading assumption implies each relay in ξ has an equal chance to be selected as the best relay. To simplify the analysis, the cardinality of ξ is approximated by its mean such that

$$\Pr(R_{\bar{m}} = R_i) \approx \frac{1}{\overline{M}_e} = \frac{1}{Mv_1} \quad (30)$$

where $\overline{M}_e$ is the average number of relays in ξ and v_1 is the steady-state probability of state s_1. Combining Eqs (29) and (30), the closed-form for $P_{1,0}$ can be obtained.

The transition probability from s_1 to s_1 can be solved in the similar manner as the previous case, so the derivation is omitted.

When the two-state Markov chain is formulated, the steady-state probability vector can be easily obtained as

$$v = (v_0, v_1) = \left(\frac{p_{1,0}}{p_{0,1} + p_{1,0}}, \frac{p_{0,1}}{p_{0,1} + p_{1,0}}\right) \quad (31)$$

It should be noted that both v_0 and v_1 involve $P_{1,0}$, which is a function of v_1. By substituting $P_{0,1}$ and $P_{1,0}$ into Eq. (31), v_1 can be solved explicitly. Taking the condition $2VC < BC$ in Eq. (29), v_1 can be obtained in closed-form as

$$v_1 = 1 - \frac{2V}{BM}\left(\frac{B - V}{B} + \frac{1}{BC} \sum_{n=0}^{m_i-1} \left(\frac{1}{m_1/\overline{E}_{R_i}} - \exp\left(-\frac{m_1 VC}{\overline{\omega}_{R_i}}\right) \sum_{k=0}^{n} \frac{n!(VC)^k}{k!(m_1/\overline{\omega}_{R_i})^{1-k}}\right)\right)^{-1} \quad (32)$$

With v_1 at hand, $\Pr(|\xi| = \Omega)$ $(\Omega = 1, 2, 3, \cdots)$ can be got which follows the binomial distribution with the probability mass function given as

$$\Pr(|\xi| = \Omega) = \binom{M}{\Omega} (v_1)^{\Omega} (1 - v_1)^{M-\Omega} \quad (33)$$

where $\binom{a}{b} = \frac{a!}{(a-b)!b!}$. With the close form of $\Pr(|\xi| = \Omega)$, the performance can be analyzed in the following part.

3 Performance analysis

3.1 Outage behavior

According to the total probability law, the outage probability of D_p or D_q can be written as

$$P_{out}^{\Xi} = \sum_{\Omega=1}^{M} \Pr(|\xi| = \Omega) \tilde{P}_{out}^{\Xi, \Omega} \quad (34)$$

where $\Xi = \{p, q\}$. As $\Pr(|\xi| = \Omega)$ can be got in Eq. (33), the next step is to get $\tilde{P}_{out}^{\Gamma, \Omega}$, which will be given in the following.

The scheme would be in outage if the SINR falls below the pre-set threshold, so the outage probability of terminal D_p is given by

$$\begin{aligned}\tilde{P}_{out}^{p,\Omega} &= \Pr(\gamma_{D_p} < \gamma_{thp}) \\ &= \Pr(\max(\gamma_{SD_p}, \gamma_{R_{\bar{m}}D_p}) < \gamma_{thp}) \\ &= \underbrace{\Pr(\gamma_{SD_p} < \gamma_{thp})}_{J_1}\underbrace{\Pr(\gamma_{R_{\bar{m}}D_p} < \gamma_{thp})}_{J_2} \quad (35)\end{aligned}$$

where γ_{thp} is the threshold of D_p. Next, according to order statistics[20], PDF and CDF of the sorted random variable $\hat{G}_{SD_p}$ are expressed as

$$f_{\hat{G}_{SD_p}}(x) = \sum_{j=0}^{N-P}(-1)^j\Lambda_p^N\binom{N-P}{j}f_{G_{SD_j}}(x)(F_{G_{SD_j}}(x))^{p+j-1} \quad (36)$$

$$F_{\hat{G}_{SD_p}}(x) = \sum_{j=0}^{N-P}\frac{(-1)^j\Lambda_p^N}{p+j}\binom{N-P}{j}(F_{G_{SD_j}}(x))^{p+j} \quad (37)$$

where $\Lambda_p^N = N!/((N-p)!(p-1)!)$. With the defination of PDF and CDF of G_{SD_i}, which is similar to Eqs(21) and (22), J_1 is calculated by

$$\begin{aligned}J_1 &= \Pr\left(\frac{a_p\hat{G}_{SD_p}\gamma}{a_q\hat{G}_{SD_p}\gamma+1} < \gamma_{thp}\right) = \int_0^{\tau}f_{\hat{G}_{SD_p}}(x)\mathrm{d}x \\ &= \sum_{j=0}^{N-p}\Lambda_p^N\frac{(-1)^j}{p+j}\binom{N-p}{j} \\ &\quad\times\left(1-\exp\left(-\frac{m_0\tau}{\Phi_{SD}}\right)\sum_{n=0}^{m_0-1}\frac{(m_0\tau/\Phi_{SD})^n}{n!}\right)^{p+j}\end{aligned} \quad (38)$$

where $\tau = \gamma_{thp}/\gamma(a_p - a_q\gamma_{thp})$. It is noteworthy that Eq. (38) exists if and only if $\gamma_{thp} < a_p/a_q$, otherwise the probability will be always one. With the help of Eqs(36) and (37), J_2 can be simplified as

$$\begin{aligned}J_2 &= \Pr(G_{R_{\bar{m}}D_p} \leqslant \tau) + \\ &\Pr\left(G_{R_{\bar{m}}D_p} > \tau, G_{SR_{\bar{m}}} \leqslant \frac{\tau(\gamma G_{R_{\bar{m}}D_p}\gamma_{\bar{m}} + \gamma G_{R_{\bar{m}}D_p} + \gamma_{\bar{m}} + 1)}{\gamma(G_{R_{\bar{m}}D_p} - \tau)}\right) \\ &= \int_0^{\tau}f_{G_{R_{\bar{m}}D_p}}(x)\mathrm{d}x \\ &\quad + \int_{\tau}^{\infty}f_{G_{R_{\bar{m}}D_p}}(y)\mathrm{d}y\int_0^{\frac{\tau(\gamma y\gamma_{\bar{m}}+\gamma y+\gamma_{\bar{m}}+1)}{\gamma(y-\tau)}}f_{G_{SR_{\bar{m}}}}(x)\mathrm{d}x\end{aligned} \quad (39)$$

To solve Eq. (39), $f_{G_{SR_{\bar{m}}}}(x)$ needs to be calculated first, which can be got according to Eq. (36) when $P=1$ and $N=\Omega$. The deifnation of $f_{G_{R_{\bar{m}}D_p}}(y)$ is similar to Eq. (21). With the help of Ref. [19] and using $f_{G_{SR_{\bar{m}}}}(x)$ and $f_{G_{R_{\bar{m}}D_p}}(y)$, J_2 can be formulated as

$$\begin{aligned}J_2 &= 1 - \exp\left(-\frac{m_2\tau}{\Phi_{RD}}\right)\sum_{n=0}^{m_2-1}\frac{(m_2\tau/\Phi_{RD})^n}{n!} \\ &\quad + \frac{\Lambda_1^{\Omega}}{\Gamma(m_2)}\left(\frac{m_2}{\Phi_{RD}}\right)^{m_2}\exp\left(-\frac{m_2\tau}{\Phi_{RD}}\right) \\ &\quad\times\sum_{j=0}^{\Omega-1}\frac{(-1)^j}{j+1}\binom{\Omega-1}{j}\sum_{r=0}^{j}(-1)^r\exp\left(-\frac{m_1ru_{\bar{m}}}{\Phi_{SR}}\right) \\ &\quad\times\sum_{r_i\geq 0, r_0+r_1+\cdots+r_{m_1-1}=r}\frac{\binom{r}{r_0, r_1, \cdots, r_{m_1-1}}\left(\frac{m_1u_{\bar{m}}}{\Phi_{SR}}\right)^{\sum_{z=0}^{m_1-1}zr_z}}{\prod_{z=0}^{m_1-1}(z!)^{r_z}} \\ &\quad\times\sum_{k_1=0}^{\sum_{z=0}^{m_1-1}zr_z}\sum_{k_2=0}^{m_2-1}\tau^{m_2-1-k_2}2\binom{\sum_{z=0}^{m_1-1}zr_z}{k_1}\binom{m_2-1}{k_2} \\ &\quad\times d^{k_1}\tau^{m_2-1-k_2}\left(\frac{m_1ru_{\bar{m}}d\Phi_{RD}}{\Phi_{SR}m_2}\right)^{\frac{k_2-k_1+1}{2}}K_{k_2-k_1+1}\left(\sqrt{\frac{2m_1ru_{\bar{m}}dm_2}{\Phi_{SR}\Phi_{RD}}}\right)\end{aligned} \quad (40)$$

where $u_{\bar{m}} = \tau(\gamma_{\bar{m}} + 1)$, $d = \tau + 1/\gamma$, $\binom{r}{r_0, r_1, \cdots, r_{m_1-1}} = \frac{r!}{r_0!r_1!\cdots r_{m_1-1}!}$, $\sum_{r_i\geq 0,\ r_0+r_1+\cdots+r_{m_1-1}=r}$ means the sum of all the possible values of which satisfies $r_0 + r_1 + \cdots + r_{m_1-1} = r$ and $K_v(\cdot)$ expresses the vth-order modified Bessel function of the second kind[19]. By substituting Eqs(33), (38) and (40) into Eq. (34), the outage probability of D_p can be obtained.

Next, the analysis of an outage event at D_q is presented. Owing to the mechanism of SIC, the outage probability of D_q is given in the following.

$$\begin{aligned}P_{out}^{q} &= \Pr(\gamma_{D_q} < \gamma_{thq}) \\ &= \Pr(\gamma_{SD_q} < \gamma_{thq})\Pr(\gamma_{R_{\bar{m}}D_q} < \gamma_{thq}) \\ &= \underbrace{(1 - \Pr(\gamma_{SD_{q\to p}} \geqslant \gamma_{thp})\Pr(\gamma_{SD_q} \geqslant \gamma_{thq}))}_{J_3} \\ &\quad\times\underbrace{(1 - \Pr(\gamma_{R_{\bar{m}}D_{q\to p}} \geqslant \gamma_{thp})\Pr(\gamma_{R_{\bar{m}}D_q} \geqslant \gamma_{thq}))}_{J_4}\end{aligned} \quad (41)$$

where γ_{thq} is the threshold of D_q. J_3 can be expanded as

$$\begin{aligned}J_3 &= 1 - \Pr\left(\frac{a_p\gamma\hat{G}_{SD_q}}{a_q\gamma\hat{G}_{SD_q}+1} \geqslant \gamma_{thp}\right)\Pr(\gamma a_q\hat{G}_{SD_q} \geqslant \gamma_{thq}) \\ &= 1 - \Pr\left(\hat{G}_{SD_q} \geqslant \max\left(\frac{\gamma_{thp}}{\gamma(a_p - a_q\gamma_{thp})}, \frac{\gamma_{thq}}{\gamma a_q}\right) \triangleq \beta\right) \\ &= \sum_{j=0}^{N-q}\Lambda_p^N\frac{(-1)^j}{q+j}\binom{N-q}{j} \\ &\quad\times\left(1-\exp\left(-\frac{m_0\beta}{\Phi_{SD}}\right)\sum_{n=0}^{m_0-1}\frac{(m_0\beta/\Phi_{SD})^n}{n!}\right)^{q+j}\end{aligned} \quad (42)$$

Next, according to Eqs(13) and (15), J_4 can be written as

$$\begin{aligned}J_4 &= 1 - \int_{\beta}^{\infty}\int_{\frac{\beta(\gamma y\gamma_{\bar{m}}+\gamma y+\gamma_{\bar{m}}+1)}{\gamma(y-\beta)}}^{\infty}f_{G_{SR_{\bar{m}}}}(x)f_{G_{R_{\bar{m}}D_q}}(y)\mathrm{d}x\mathrm{d}y \\ &= \int_0^{\beta}f_{G_{R_{\bar{m}}D_q}}(y)\mathrm{d}y + \int_{\beta}^{\infty}f_{G_{R_{\bar{m}}D_q}}(y)\mathrm{d}y\int_0^{\frac{\beta(\gamma y\gamma_{\bar{m}}+\gamma y+\gamma_{\bar{m}}+1)}{\gamma(y-\beta)}}f_{G_{SR_{\bar{m}}}}(x)\mathrm{d}x\end{aligned} \quad (43)$$

The derivation of the integral in Eq. (43) is the same as Eq. (39), so it is omitted here. So far, the outage probability of D_q has been derived by substituting Eqs(33), (42) and (43) into Eq. (34).

3.2 Ergodic sum-rate

In this section, the ergodic sum-rate for a pair of users is analysed which is given by

$$\begin{aligned} R_{sum} &= R_{ave}^{p} + R_{ave}^{q} \\ &= E(\log_2(1+\gamma_{D_p})) + E(\log_2(1+\gamma_{D_q})) \end{aligned} \tag{44}$$

The rate of D_p can be calculated in the following, where approximation is attained under the condition of $\gamma \to \infty$.

$$\begin{aligned} R_{ave}^{p} &= E(\log_2(1+\gamma_{D_p})) \\ &= E(\log_2(1+\max(\gamma_{SD_p}, \gamma_{R_{\bar{m}}D_p}))) \\ &\approx E\left(\log_2\left(1+\max\left(\frac{a_p}{a_q}, \frac{a_p\gamma G_{SR_{\bar{m}}}}{a_q\gamma G_{SR_{\bar{m}}}}\right)\right)\right) \\ &= \log_2\left(\frac{a_p}{a_q}\right) \end{aligned} \tag{45}$$

The rate of D_q can be calculated as

$$\begin{aligned} R_{ave}^{q} &= E(\log_2(1+\gamma_{D_q})) \\ &= \Pr(\gamma_{SD_{q\to p}} \geqslant \gamma_{thp})\Pr(\gamma_{R_{\bar{m}}D_{q\to p}} \leqslant \gamma_{thp}) \\ &\quad \times \underbrace{E(\log_2(1+\gamma_{SD_q}))}_{J_5} \\ &\quad + \Pr(\gamma_{SD_{q\to p}} \leqslant \gamma_{thp})\Pr(\gamma_{R_{\bar{m}}D_{q\to p}} \leqslant \gamma_{thp}) \\ &\quad \times \underbrace{E(\log_2(1+\gamma_{R_{\bar{m}}D_q}))}_{J_6} \\ &\quad + \Pr(\gamma_{SD_{q\to p}} \geqslant \gamma_{thp})\Pr(\gamma_{R_{\bar{m}}D_{q\to p}} \leqslant \gamma_{thp}) \\ &\quad \times \underbrace{E(\log_2(1+\max(\gamma_{SD_q}, \gamma_{R_{\bar{m}}D_q})))}_{J_7} \end{aligned} \tag{46}$$

All probabilities in the Eq. (46) can be got according to the above analysis. Only J_5, J_6 and J_7 need to be derived in the following. Firstly, J_5 can be written as

$$\begin{aligned} J_5 &= E\left(\frac{1}{\ln 2}\ln(1+a_q\hat{G}_{SD_q}\gamma)\right) \\ &= \frac{1}{\ln 2}\int_0^{\infty}\ln(1+a_q\gamma x) f_{\hat{G}_{SD_q}}(x)\,\mathrm{d}x \\ &= \frac{1}{\ln 2}\int_0^{\infty}\frac{1-F_{\hat{G}_{SD_q}}(x/a_q\gamma)}{1+x}\mathrm{d}x \end{aligned} \tag{47}$$

Using Eq. (37), Eq. (3.351.2) of Ref. [19] and Eq. (3.353.5) in Ref. [19], the close form of J_5 can be got as

$$\begin{aligned} J_5 = {} & \frac{\Lambda_q^N}{\ln 2\,\Gamma(m_0)}\sum\nolimits_{j=0}^{N-q}(-1)^j\binom{N-q}{j} \\ & \times \sum\nolimits_{r=0}^{q+j-1}\sum_{r_i\geqslant 0,\ r_0+r_1+\cdots+r_{m_2-1}=r}(-1)^r \\ & \times \frac{\binom{r}{r_0, r_1, \cdots, r_{m_2-1}}}{\prod\nolimits_{z=0}^{m_2-1}(z!)^{r_z}}\left(\sum\nolimits_{z=0}^{m_0-1}zr_z + m_0 - 1\right)! \\ & \times \sum\nolimits_{t=1}^{\sum_{z=0}^{m_0-1}zr_z+m_0-1}\frac{\Phi_{SD}^{-t}}{t!(a_q\gamma)^t m_0^{-t}(r+1)^{\sum_{z=0}^{m_0-1}zr_z+m_0-t}} \\ & \times \left((-1)^{t-1}\exp\left(\frac{m_0(r+1)}{a_q\gamma\Phi_{SD}}\right)Ei\left(-\frac{m_0(r+1)}{a_q\gamma\Phi_{SD}}\right)\right. \\ & \left. + \sum\nolimits_{o=1}^{t}(o-1)!(-1)^{t-o}\left(\frac{m_0(r+1)}{a_q\gamma\Phi_{SD}}\right)^{-o}\right) \end{aligned} \tag{48}$$

where $Ei(x) = \int_x^{\infty} t^{-1}\exp(-t)\,\mathrm{d}t$ denotes the exponential integral function Eq. (5.1.1) in Ref. [19]. Secondly, in order to calculate J_6, the asymptotic expression can be obtained as

$$\begin{aligned} & J_6 \\ & = E\left(\log_2\left(1+\frac{a_q\gamma^2 G_{SR_{\bar{m}}}G_{R_{\bar{m}}D_q}}{\gamma(G_{SR_{\bar{m}}}+G_{R_{\bar{m}}D_q})+\gamma G_{R_{\bar{m}}D_q}\gamma_{\bar{m}}+\gamma_{\bar{m}}+1}\right)\right) \\ & = E\left(\log_2\left(1+\frac{a_q\gamma^2\dfrac{G_{SR_{\bar{m}}}}{\gamma_{\bar{m}}+1}G_{R_{\bar{m}}D_q}}{\dfrac{\gamma G_{SR_{\bar{m}}}}{\gamma_{\bar{m}}+1}+\gamma G_{R_{\bar{m}}D_q}+1}\right)\right) \\ & < E\left(\log_2\left(1+a_q\gamma\min\left(G_{R_{\bar{m}}D_q}, \frac{G_{SR_{\bar{m}}}}{\gamma_{\bar{m}}+1}\right)\right)\right) \end{aligned} \tag{49}$$

Now denoting the random variable:

$$L = a_q\gamma\min\left(G_{R_{\bar{m}}D_q}, \frac{G_{SR_{\bar{m}}}}{\gamma_{\bar{m}}+1}\right) \tag{50}$$

Thus an upper bound of J_6 is rewritten as

$$J_6 < E\left(\frac{1}{\ln 2}\ln(1+l)\right) = \frac{1}{\ln 2}\int_0^{\infty}\frac{1-F_L(l)}{1+l}\mathrm{d}l \tag{51}$$

Submitting the PDFs of $G_{SR_{\bar{m}}}$ and $G_{R_{\bar{m}}D_q}$ into Eq. (51) and using Eq. (3.353.7) in Ref. [19], J_6 can be got as

$$\begin{aligned} J_6 < {} & \frac{\Lambda_1^{\Omega}}{\ln 2\,\Gamma(m_1)}\sum_{n=0}^{m_2-1}\frac{(m_2/\Phi_{RD}a_q\gamma)^n}{n!}\sum\nolimits_{j=0}^{\Omega-1}(-1)^j \\ & \binom{\Omega-1}{j}\times\sum\nolimits_{r=0}^{j}\sum_{r_i\geqslant 0, r_0+r_1+\cdots+r_{m_1-1}=r}\frac{(-1)^r}{\prod\nolimits_{z=0}^{m_1-1}(z!)^{r_z}} \\ & \times\sum\nolimits_{o=0}^{\sum_{z=0}^{m_1-1}zr_z+m_1-1}\frac{\left(\sum\nolimits_{z=0}^{m_1-1}zr_z+m_1-1\right)!(\gamma_{\bar{m}}+1)^o\Phi_{SR}^{-o}}{o!(a_q\gamma)^o(r+1)^{\sum_{z=0}^{m_1-1}zr_z+m_1-o}m_1^{-o}} \\ & \times\left((-1)^{n+o-1}\exp\left(\frac{m_1(\gamma_{\bar{m}}+1)(r+1)}{\Phi_{SR}a_q\gamma}+\frac{m_2}{a_q\gamma\Phi_{RD}}\right)\right. \\ & \times Ei\left(-\frac{m_1(\gamma_{\bar{m}}+1)(r+1)}{\Phi_{SR}a_q\gamma}-\frac{m_2}{a_q\gamma\Phi_{RD}}\right)+\sum\nolimits_{\varepsilon=1}^{n+o} \\ & \left.(\varepsilon-1)!(-1)^{n+o-\varepsilon}\left(\frac{m_1(\gamma_{\bar{m}}+1)(r+1)}{\Phi_{SR}a_q\gamma}+\frac{m_2}{a_q\gamma\Phi_{RD}}\right)^{-\varepsilon}\right) \end{aligned} \tag{52}$$

Thirdly, J_7 can be rewritten as

$$\begin{aligned} J_7 &= E(\log_2(1 + \max(\gamma_{SD_q}, \gamma_{RD_q}))) \\ &= E\left(\log_2\left(1 + \max\left(a_q\gamma\hat{G}_{SD_q}, \frac{a_q\gamma^2 \dfrac{G_{SR_{\bar{m}}}}{\gamma_{\bar{m}} + 1} G_{R_{\bar{m}}D_q}}{\gamma \dfrac{G_{SR_{\bar{m}}}}{\gamma_{\bar{m}} + 1} + \gamma G_{R_{\bar{m}}D_q} + 1}\right)\right)\right) \\ &< E\left(\log_2\left(1 + \max\left(a_q\gamma\hat{G}_{SD_q}, a_q\gamma\min\left(\frac{G_{SR_{\bar{m}}}}{\gamma_{\bar{m}} + 1}, G_{R_{\bar{m}}D_q}\right)\right)\right)\right) \end{aligned} \tag{53}$$

As the derivation process of Eq. (49), denoting the random variable

$$W = a_q\gamma\max\left(\hat{G}_{SD_q},\ \min\left(\frac{G_{SR_{\bar{m}}}}{\gamma_{\bar{m}} + 1},\ h_{R_{\bar{m}}D_q}\right)\right) \tag{54}$$

Then, Eq. (53) can be written as

$$J_7 < E\left(\frac{B}{\ln 2}\ln(1 + W)\right) = \frac{B}{\ln 2}\int_0^{\infty} \frac{1 - F_W(w)}{1 + w}\mathrm{d}w \tag{55}$$

The derivation of Eq. (55) is the same as Eq. (51), so it is omitted here. By Submitting Eqs(48), (52), (55) and all the probabilities into Eq. (46), the closed-form expression of R_{ave}^q can be got. With the R_{ave}^p and R_{ave}^q, the expression of R_{sum} can be obtianed.

4 Results and discussion

In this section, Monto-Carlo simulations are performed to validate the theoretical analysis. In all simulations, the energy conversion efficiency $\eta = 0.5$, the fixed transmission rate of the source is 1 bit per channel use (bpcu). C is set as the multiple of the source transmission energy, i. e., $C = \delta PT$, where $\delta > 0$ is the scaling factor. To facilitate the analysis, the following sets of parameters are used: $N = 3$, $\sigma^2 = 1$, $m_0 = m_1 = m_2 = 2$, $\Phi_{SD} = \Phi_{SR} = \Phi_{RD} = 1$, $a_p = 8/9$, $a_q = 1/9$, $\gamma_{thp} = 1$ dB, $\gamma_{thq} = 2$ dB, $p = 1$, $q = 3$.

Fig. 2 shows the performance of the proposed scheme and existing schemes versus the transmitting SNR of source. One relay is sleceted randomly from the eligible relay set when the FD-NOMA (random) scheme is used. It can be seen that the approximate analysis of finite Markov chain is accurate in the whole SNRs. Compared with the HD-NOMA, FD-NOMA (random) and conventional OMA relaying scheme, the outage behavior of each terminal in the FD-NOMA relaying system is better, even in the existence of SI at the relay. It can also be found that the diversity order for each user in the proposed shceme is equal to that in the HD cooperative NOMA system. Since the theoretical analyses agree well with the simulations, only analytical results will be plotted in the remaining outage probability figures.

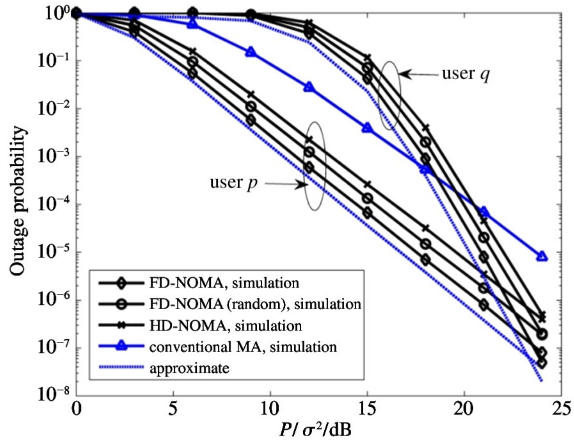

(SI = −10 dB, $\delta = 0.5$, $M = 6$, $B = 10$)

Fig. 2 Outage probability with different user and scheme

In Fig. 3, the impacts of SI on the outage probability are investigated. It can be seen that the outage performance of the FD relaying (only take one user, e. g., D_p, and vice versa) system will become worse than that in the HD relaying network for high-SNR values when SI is extremely severe. But both two schemes can have better outage performance than the conventional OMA scheme and spectral efficiency can be improved in the FD-NOMA system.

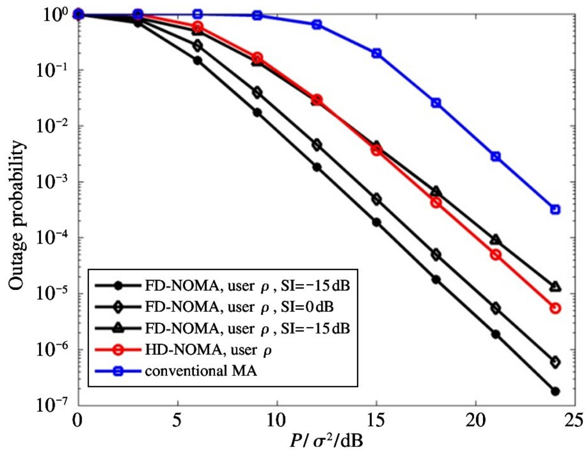

($\delta = 0.5$, $M = 6$, $B = 10$)

Fig. 3 Outage probability with different SI

In Fig. 4, the impacts of δ on the performance of the proposed scheme with different SI in medium SNR conditions ($P/\sigma^2 = 20$ dB) are illustrated. For all the curves, the trends are the same for all schemes, namely, the probability first decreases then increases as δ varies from 0 to 1. This means that, when the other parameters are determined, there must be an optimal value of δ. However, the values of the inflection points are not always the same for different users and SI. It can be seen that for the user with better channel condition (D_q), the optimal value is smaller than user with worse channel condition (D_p). This is because D_p has the worse direct link, so it needs more power to enhance the relay link. It can also be seen that for the FD cooperative NOMA system, the optimal value shifts to the left with the increase in the level of SI and when δ is too big, the outage behavior is nearly the same under different values of SI. Compared to the HD cooperative NOMA system, the outage behavior of D_p is getting inferior when the value of SI is large and δ is small. Finally, the optimal value of δ can easily be obtained by a one-dimensional exhaustive search. With this optimal value of δ, the system can resist fading more effectively.

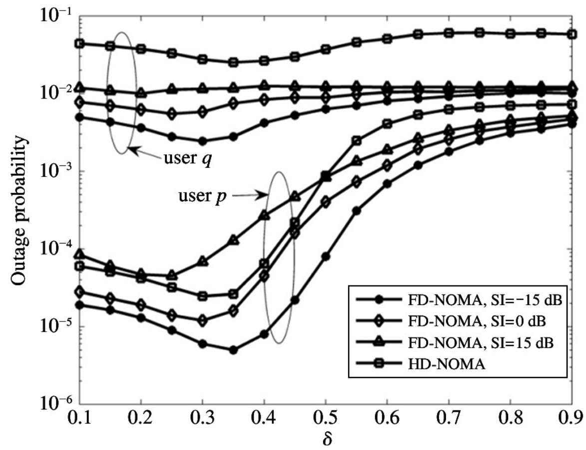

Fig. 4 Outage probability against δ ($M = 6$, $B = 10$)

Fig. 5 presents the rates of the two paired terminals varies with system SNR. Firstly, the ergodic sum-rate increases with the growth of transmitting SNR, and asymptotic curves of the ergodic sum-rate and simulation results are almost overlapping in the medium- and high-SNR regions, we will only plot the analytical results in the remaining rate figures. Secondly, the results clearly show that the FD-NOMA system can achieve a larger sum-rate compared with the HD relaying system, FD-NOMA (random) and conventional OMA system, but twice as much as HD-NOMA cannot be achieved owing to the effect of SI. More importantly, with the increase of system SNR, the rate of D_p approaches a certain value, whereas the D_q can obtain improved performance. Both the two conclusions are consistent with the derivations in Eq. (45) and Eq. (46).

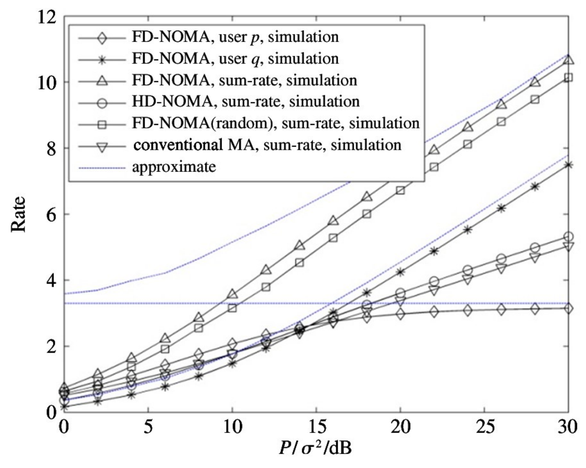

(SI = −15 dB, $\delta = 0.5$, $M = 6$)

Fig. 5 Rate with different user and different scheme

In Fig. 6, the impact of battery size on the proposed finite battery scheme is investigated by varying the relay number and SI. It can be observed that the performance increases as B or relay number increase. However, the gain provided by a larger battery size does not increase when B exceeds a certain value and this value is approximate to 6. From this figure, it can also be seen that the battery can not offer enough energy for forwarding the data when $B = 1$, so the performances are the same for all curves and the performance gap for different SI increases as the number of relay increases.

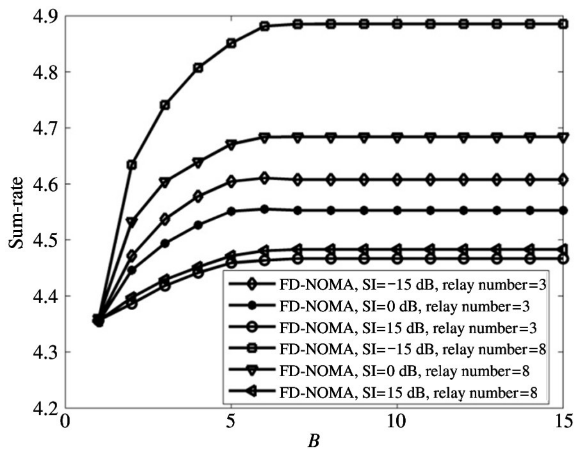

Fig. 6 Sum-rate against B ($\delta = 0.5$)

5 Conclusions

A relay selection scheme for the FD-NOMA networks with EH over Nakagami-m fading channels has been proposed. The amount of harvested energy at each relay is modeled as a finite Markov chain and then the approximate closed-form expression of the outage probability and ergodic sum-rate are derived. Simulations are carried out to verify the effectiveness of the theoretical analysis. It is concluded that through carefully choosing the system parameters of the network, (e. g., EH threshold), FD-NOMA performs much better than the HD-NOMA or the conventional OMA.

References

[1] Qin Z J, Yue X W, Liu Y W, et al. User association and resource allocation in unified NOMA enabled heterogeneous ultra dense networks [J]. *IEEE Communications Magazine*, 2018, 56(6): 86-92

[2] Xiao K, Gong L, Kadoch M. Opportunistic multicast NOMA with security concerns in a 5G massive MIMO system [J]. *IEEE Communications Magazine*, 2018, 56 (3): 91-95

[3] Ding Z G, Peng M G, Poor H V. Cooperative non-orthogonal multiple access in 5G systems[J]. *IEEE Communications Letters*, 2015, 19(8): 1462-1465

[4] Liang X S, Wu Y P, Ng D W K, et al. Outage performance for cooperative NOMA transmission with an AF relay [J]. *IEEE Communications Letters*, 2017, 21 (11): 2428-2431

[5] Zhang Z S, Chai X M, Long K P, et al. Full duplex techniques for 5G networks: self-interference cancellation, protocol design, and relay selection [J]. *IEEE Communications Magazine*, 2015, 53(5): 128-137

[6] Wang Q, Dong Y, Xu X D, et al. Outage probability of full-duplex AF relaying with processing delay and residual self-interference [J]. *IEEE Communications Letters*, 2015, 19 (5): 783-786

[7] Osorio D P M, Olivo E E. B, Alves H, et al. Exploiting the direct link in full-duplex amplify-and-forward relaying networks [J]. *IEEE Signal Processing Letters*, 2015, 22 (10): 1766- 1770

[8] Kwon T, Lim S, Choi S, et al. Optimal duplex mode for DF relay in terms of the outage probability [J]. *IEEE Transactions on Vehicular Technology*, 2010, 59 (7): 3628-3634

[9] Hossain E, Rasti M, Tabassum H, et al. Evolution toward 5G multi-tier cellular wireless networks: an interference management perspective [J]. *IEEE Wireless Communications*, 2014, 21 (3): 118-127

[10] Nasir A A, Zhou X Y, Durrani S, et al. Relaying protocols for wireless energy harvesting and information processing [J]. *IEEE Transactions on Wireless Communications*, 2013, 12(7): 3622-3636

[11] Hoang T M, Nguyen B C, Tran P T, et al. Outage analysis of RF energy harvesting cooperative communication systems over Nakagami-*m* fading channels with integer and non-integer *m* [J]. *IEEE Transactions on Vehicular Technology*, 2020, 69(3): 2785-2801

[12] Chatterjee S, Maity S P, Acharya T. Energy-spectrum efficiency trade-off in energy harvesting cooperative cognitive radio networks [J]. *IEEE Transactions on Cognitive Communications and Networking*, 2019, 5(2): 295-303

[13] Sudevalayam S, Kulkarni P. Energy harvesting sensor nodes: survey and implications [J]. *IEEE Communications Surveys and Tutorials*, 2011, 13(3): 443-461

[14] Zhou Z, Peng M G, Zhao Z Y, et al. Wireless-powered cooperative communications: power-splitting relaying with energy accumulation[J]. *IEEE Journal on Selected Areas in Communications*, 2016, 34(4): 969-982

[15] Guo W D, Tian H Y. Cooperative non-orthogonal multiple access with energy harvesting [J]. *Information*, 2017, 8(3): 1-15

[16] Zhang Z Q, Ma Z, Ding Z G, et al. Full-duplex two-way and one-way relaying: average rate, outage probability, and tradeoffs[J]. *IEEE Transactions on Wireless Communications*, 2016, 15(6): 3920-3933

[17] Yue X W, Liu Y W, Kang S L, et al. Exploiting full/half-duplex user relaying in NOMA systems [J]. *IEEE Transactions on Communications*, 2018, 66(2): 560-575

[18] Rego V. Characterization of equilibrium queue length distributions in M/GI/I queues[J]. *Computers and Operations Research*, 1988, 15: 7-17

[19] Gradshteyn I, Ryzhik I. Table of Integrals, Series and Products [M]. San Diego: Academic Press, 1994

[20] David H A, Nagaraja H N. Order Statistics [M]. New York: John Wiley, 2003

Guo Weidong, born in 1982. He received his Ph. D degree in Communication and Information System from Shandong University in 2012. He also received his B. E. and M. S. degrees from Hohai University in 2005 and 2008 respectively. He is currently working at the School of Cyber Science and Engineering of Qufu Normal University. His research interests include non-orthogonal multiple access, energy harvesting and network security.